

## RESEARCH ARTICLE

# A deep-learning artificial intelligence system for assessment of root morphology of the mandibular first molar on panoramic radiography

<sup>1</sup>Teruhiko Hiraiwa, <sup>1</sup>Yoshiko Arijii, <sup>1</sup>Motoki Fukuda, <sup>1</sup>Yoshitaka Kise, <sup>2</sup>Kazuhiko Nakata, <sup>3</sup>Akitoshi Katsumata, <sup>4</sup>Hiroshi Fujita and <sup>1</sup>Eiichiro Arijii

<sup>1</sup>Department of Oral and Maxillofacial Radiology, Aichi-Gakuin University School of Dentistry, Nagoya, Japan; <sup>2</sup>Department of Endodontics, Aichi-Gakuin University School of Dentistry, Nagoya, Japan; <sup>3</sup>Department of Oral Radiology, Asahi University School of Dentistry, Mizuho, Japan; <sup>4</sup>Department of Electrical, Electronic and Computer Faculty of Engineering, Gifu University, Gifu, Japan

**Objectives:** The distal root of the mandibular first molar occasionally has an extra root, which can directly affect the outcome of endodontic therapy. In this study, we examined the diagnostic performance of a deep learning system for classification of the root morphology of mandibular first molars on panoramic radiographs. Dental cone-beam CT (CBCT) was used as the gold standard.

**Methods:** CBCT images and panoramic radiographs of 760 mandibular first molars from 400 patients who had not undergone root canal treatments were analyzed. Distal roots were examined on CBCT images to determine the presence of a single or extra root. Image patches of the roots were segmented from panoramic radiographs and applied to a deep learning system, and its diagnostic performance in the classification of root morphology was examined.

**Results:** Extra roots were observed in 21.4% of distal roots on CBCT images. The deep learning system had diagnostic accuracy of 86.9% for the determination of whether distal roots were single or had extra roots.

**Conclusions:** The deep learning system showed high accuracy in the differential diagnosis of a single or extra root in the distal roots of mandibular first molars.

*Dentomaxillofacial Radiology* (2019) **48**, 20180218. doi: [10.1259/dmfr.20180218](https://doi.org/10.1259/dmfr.20180218)

**Cite this article as:** Hiraiwa T, Arijii Y, Fukuda M, Kise Y, Nakata K, Katsumata A, et al. A deep-learning artificial intelligence system for assessment of root morphology of the mandibular first molar on panoramic radiography. *Dentomaxillofac Radiol* 2019; **48**: 20180218.

**Keywords:** artificial intelligence; deep learning; mandibular first molar; panoramic radiography; root morphology

## Introduction

The mandibular first molar is usually the first permanent tooth to erupt, and has a high risk of decay and subsequent pulp damage: thus, this tooth frequently requires endodontic treatment.<sup>1,2</sup> The success of endodontic treatment depends on various factors,<sup>3</sup> and the anatomical configuration of the root and root canal make up one such essential factor,<sup>4,5</sup> because a canal that is overlooked and goes untreated may provoke microbial

colonization resulting in treatment failure.<sup>2,3</sup> In Japanese and Chinese populations, the incidence of an extra root in the distal root is reported to be relatively high (more than 20%).<sup>2,6</sup>

Nowadays, such variations in the root and canal morphology can be accurately evaluated in the clinics using cone-beam CT (CBCT) for dental use.<sup>1-3,7,8</sup> Although conventional radiography is widely applied and still has an essential role in the diagnosis and treatment planning for root canal pathologies,<sup>5</sup> CBCT

Correspondence to: Dr Yoshiko Arijii, [yoshiko@dpc.agu.ac.jp](mailto:yoshiko@dpc.agu.ac.jp)

Received 04 June 2018; revised 16 October 2018; accepted 19 October 2018

provides high-quality three-dimensional images,<sup>1,2,7,8</sup> thereby overcoming the limitations of conventional radiographs such as distortion and superimposition of bony and dental structures.<sup>1,4,5,7,9</sup> However, a CBCT examination results in a relatively high radiation dose to the patient in comparison with that from conventional radiography.<sup>10</sup> Therefore, it should not always be applied to patients. Panoramic radiography is one of the most popular radiographic examinations, and it would be effective for screening if all the possible variations of the root and root canal configurations could be identified, as some may be difficult to treat.

In recent years, deep learning system which is one of artificial intelligence methods has been introduced for various clinical tasks.<sup>11</sup> Deep learning systems can classify datasets automatically, and with the use of multi-layer convolutional neural networks (CNN) they can deeply-learn the features contained within data.<sup>12</sup> They have been used effectively for image-based automated diagnosis in various fields, including, lung cancer,<sup>11,13</sup> colorectal polyps,<sup>14</sup> prostate cancer,<sup>15</sup> hip osteoarthritis,<sup>12</sup> and bone age assessment.<sup>16</sup> When training image datasets are input into a deep learning system, the learning procedures are repeated automatically, without requiring manual definition of the imaging characteristics of the lesions.<sup>17</sup> In this way, deep learning methods are able to learn adaptive image features and simultaneously perform image classification.<sup>15</sup>

The purpose of the present study was to verify the diagnostic performance of a deep learning system applied to panoramic radiographs for assessing the number of the distal roots of mandibular first molars, using CBCT classification as a gold standard.

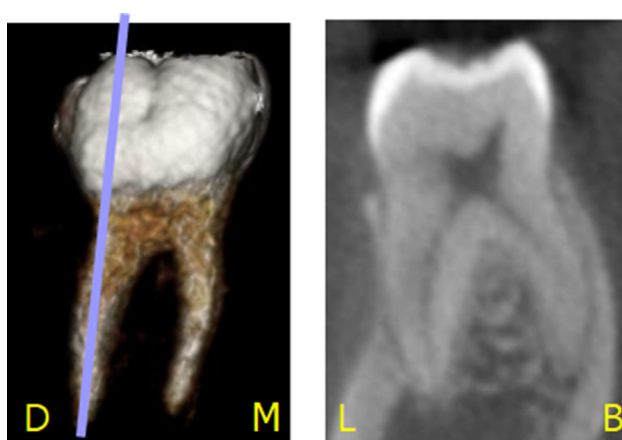
## Methods and materials

### Subjects

Subjects were retrospectively selected from an image database of patients who visited our institution between April 2017 and July 2018. Patients who underwent dental cone-beam CT (*i.e.* CBCT) and panoramic radiography, and who had not undergone root canal treatments, were identified. The patients had undergone CBCT examination for other purposes, such as impacted teeth, mandibular deformity, and cysts in other teeth. Those cases in which the mandibular first molars were included within the scanning range were selected. Patients were consecutively collected retroactively from July 2018. The patient cohort consisted of 200 males and 200 females, with an age range of 18 to 49 years (median 26.0 years). The images of 760 mandibular first molars from these patients were used in the evaluations in this study.

This study was approved by the ethics committee of our University (No. 496), and was performed in accordance with the Declaration of Helsinki.

CBCT images were taken with an Alphard Vega scanner (Asahi Roentgen Ind. Co. Ltd., Kyoto, Japan) using D-mode (51 × 51 mm) or I-mode (102 × 102



### Right first molar

**Figure 1** Methods for the reconstruction of a CBCT image The reconstructed coronal image displays the tooth in a bucco-lingual direction, and indicates an extra root in the distal root. D, distal; M, mesial; L, Lingual; B, Buccal.

mm) imaging, with voxel sizes of 0.1 or 0.2 mm respectively. The CBCT scans were performed with a rotation of 360° and exposure factors of 80 kV, 8 mA, and 17 s. Panoramic images were obtained using a Veraview epos system (J. Morita Mfg Corp., Kyoto, Japan) with the standard parameters, including a tube voltage of 75 kV, tube current of 9 mA, and acquisition time of 16 s.

### Assessment of the number of distal roots of mandibular first molars on dental CBCT images

Determination of whether distal roots were simple or were accompanied by extra roots was performed on axial, coronal, sagittal, and three-dimensional CBCT images, with the reconstructed images being prepared using the Aquarius NET software program (TeraRecon Inc., Tokyo, Japan). **Figure 1**, which shows a reconstructed coronal image, displays the tooth in a bucco-lingual direction, and indicates to the presence of an extra root in the distal root. Observations were performed by a radiologist (TH) on a 20.1 inch RadiForce G20 monitor (Eizo Nanao Corp., Ishikawa, Japan) with a resolution of 1600 × 1200 pixels.

Prior to the observation, the intraclass correlation for the evaluation of the number of distal roots was examined. One observer evaluated this for 40 teeth at a monthly interval. The resulting intraclass correlation coefficient was 1.000.

The CBCT evaluation of the distal roots of 760 mandibular first molars revealed that 597 teeth (78.6%) had single roots and 163 teeth (21.4%) had extra roots.

### Assessment of the number of distal roots of mandibular first molars on panoramic radiograms according to the deep learning system

**Preparation of image patches:** The diagnostic performance of the deep learning system using panoramic

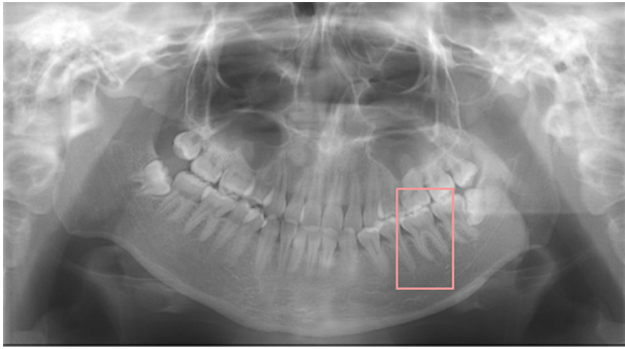


**Figure 2** Segmentation of the mandibular first molar on a panoramic radiograph. A single radiologist segmented each of the mesial and distal roots of the mandibular first molars using an image patch size of  $70 \times 120$ -pixels.

radiographs was investigated in respect to its ability to determine whether a distal root was a single root or was accompanied by an extra root. The results of the number of distal roots on CBCT were used as the gold standard.

As a first step for the deep learning study, we prepared  $70 \times 120$ -pixel image patches. The panoramic radiographs were downloaded in Bitmap form (.BMP) from the image database of our hospital, and a radiologist segmented the distal roots of the right and left mandibular first molars using  $70 \times 120$ -pixel rectangles (Figure 2).

*Five-fold cross-validation and data augmentation*

In the next preparatory step, a five-fold cross-validation procedure was performed. This procedure is a method devised for overcoming deviations in the datasets used to train a deep learning model for image classification (Figure 3).<sup>11,12,14</sup> The datasets were randomly split into five partitions, with one partition being used as a

testing dataset and the other four partitions being used as training dataset. Each partition was used once as the testing set, allowing five-fold cross-validation. This meant that in the single root group, 119 and 478 image patches per fold were used as testing and training datasets, respectively, while in the extra root group, 32 and 131 image patches per fold were used as testing and training samples. Care was taken to ensure that the training and testing data did not contain samples from the same tooth or the same patient.

The training image patches were enhanced in number by a data augmentation process. This procedure is frequently used for deep learning systems with a small number of clinical cases, and involves the data being synthetically increased in number by altering the brightness, contrast, rotation, and sharpness of the images.<sup>10,11,13</sup> Ultimately, 11,472 and 11,004 training image patches per fold were created for the single and extra root groups respectively.

For each fold, 32 image patches from the single root group and 32 from the extra root group were used as testing datasets, to maintain a balanced number of images for each classification.

*Construction of the deep learning system*

The deep learning system was implemented on a Nvidia GeForce GTX GPU workstation with 11 GB of memory. The training and testing procedures were performed using AlexNet and GoogleNet architectures implemented with the DIGITS library on the Caffe framework. The standard DIGITS algorithm was used for deep learning. When the training image patches were input into the deep learning systems, the training process was conducted for 200 epochs, with modifying using the validation image patches. The loss of the training dataset, which represents the fit between the prediction and ground truth label, decreased over

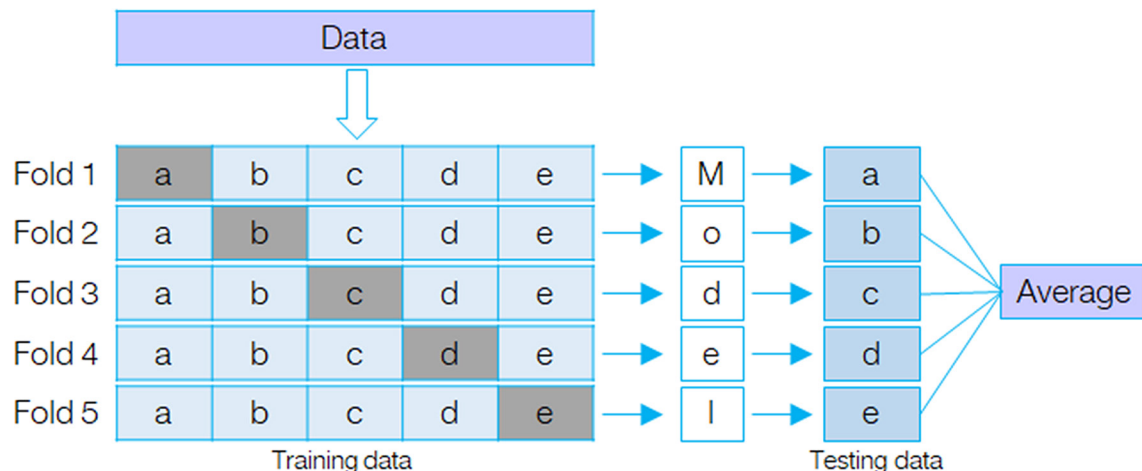


**Figure 3** Five-fold cross-validation. The data were randomly split into five partitions, with one partition being used as a testing set and the residual data being used as a training sample. A learning model was created on the basis of the training sample, and the testing data were then applied to each model. The diagnostic performance for each cross-validation set was obtained, and the average of the fivefold procedure was regarded as the estimated performance.

time as the learning improved, and the learning process was repeated until a loss became sufficiently small. As a result, the learning model was created. Human do not need to enter pre-extracted information such as imaging features in this system.

For each fold of the cross-validation, the optimal parameters for the creation of the learning model were determined on the basis of the training sample. The testing data were then applied to each model, and the classifications as to whether the distal root was single or with an extra root were performed.

For example, in the evaluation of the number of distal roots for Fold 1, 11,472 training image patches from the single root group, and 11,004 patches from the extra root group were input into the deep learning system. The learning process was performed for 200 epochs and the learning model was created. Each of the 32 testing image patches in the single and extra root group were then entered into the model, and the diagnostic performance for Fold 1 was calculated. Next, a similar process was carried out for Fold 2, using the different training and testing image patches. This process was repeated for five times.

#### Calculation of diagnostic performance

The diagnostic performance was calculated for each testing set. The average of the five-fold procedure was regarded as the performance estimate, because each cross-validation set may have been classified by slightly different optimized parameters. The accuracy, sensitivity, specificity, positive predictive value, and negative predictive value of the deep learning system using AlexNet and GoogleNet were calculated in respect to the gold standard CBCT results. The area under the curve (AUC) was also obtained from the receiver operating characteristic (ROC) analysis.

*Comparison between the deep learning system and radiologists:* The diagnostic performance of the deep learning system for determination of whether the distal roots were single or with extra roots was then compared with the performance of two radiologists. Panoramic image patches of 163 randomly-selected teeth showing

single roots and 163 teeth with extra roots were prepared. Two experienced radiologists with more than 20 years of experience examined these panoramic image patches in a random order, evaluating them for the presence of a single root or extra root. The deep learning system requires many images for the learning process, whereas the radiologists' experience in interpretation was achieved over many years. Therefore, the two experienced radiologists performed actual observations on the classification of whether the distal roots were single or with an excessive root, after training on several image patches. The accuracy, sensitivity, specificity, positive predictive value, negative predictive value, and AUC of the observers were calculated and compared with those of the deep learning system. The  $\kappa$  value for the two observers was 0.681.

*Statistical analysis:* Diagnostic performance was compared using the Mann-Whitney U Test. AUC values were compared using McNemar's chi-square analysis. The level of significance was set at  $p < 0.05$ .

## Results

#### Assessment of the number of distal roots on dental cone-beam CT images

The CBCT evaluation of the distal roots of 760 mandibular first molars revealed that 597 teeth (78.6%) had single roots and 163 teeth (21.4%) had extra roots.

#### Deep learning system assessment of the number of distal roots on panoramic radiograms

The diagnostic performance measures of the deep learning system in the determination of whether the distal root was single or with an extra root are shown in Table 1. The system using AlexNet demonstrated an accuracy of 87.4%, sensitivity of 77.3%, specificity of 97.1%, a positive predictive value of 96.3%, and a negative predictive value of 81.8%. The system using GoogleNet demonstrated an accuracy of 85.3%, sensitivity of 74.2%, specificity of 95.9%, a positive predictive value of 94.7%, and a negative predictive value of 80.0%. The system using Radiologists demonstrated an accuracy of 81.2%, sensitivity of 80.2%, specificity of 82.0%, a positive predictive value of 78.7%, and a negative predictive value of 83.4%.

**Table 1** Comparison of diagnostic performance between the deep learning system and radiologists

	Accuracy	Sensitivity	Specificity	Positive predictive value	Negative predictive value	AUC	Time for training	Time for testing
<b>AI</b>								
AlexNet	87.4	77.3	97.1	96.3	81.8	0.87	51 min	9 sec
GoogleNet	85.3	74.2	95.9	94.7	80.0	0.85	3 hr	11 sec
Radiologists	81.2	80.2	82.0	78.7	83.4	0.74	–	–
<i>p</i> values								
AI(AlexNet) vs AI(GoogleNet)	0.3991	0.5296	0.3390	0.1412	0.4647	0.0511		
AI(AlexNet) vs Radiologists	0.0528	0.4386	0.0445 <sup>a</sup>	0.0528	0.4386	<0.0001 <sup>b</sup>		
AI(GoogleNet) vs Radiologists	0.2453	0.4386	0.0424 <sup>a</sup>	0.0507	0.4386	0.0003 <sup>b</sup>		

<sup>a</sup> $p < 0.05$  (Mann-Whitney U test).

<sup>b</sup> $p < 0.01$  ( $\chi^2$ -test).



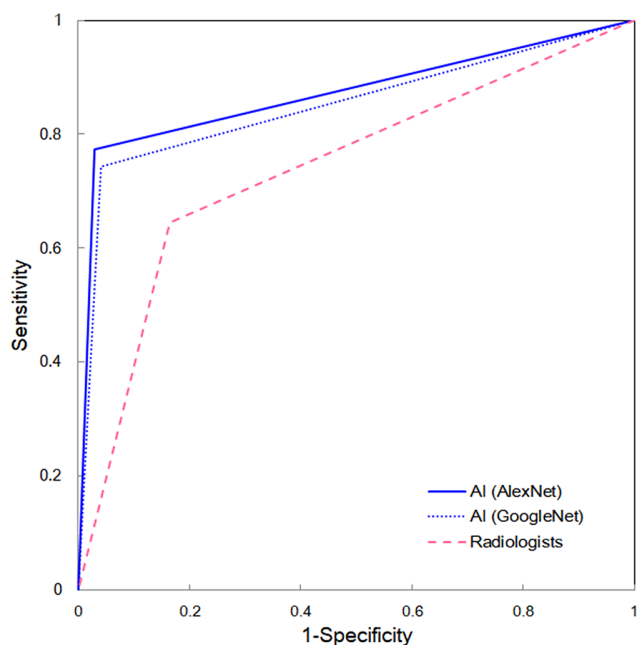


**Figure 4** Receiver operating characteristic curves for the deep learning system and the radiologists

There was no significant difference in performance between the CNNs. The time required for training from the input of the datasets to the model creation took 51 min for AlexNet and 3 h for GoogleNet. The testing times were 9 and 11 sec respectively.

#### *Comparison between the deep learning system and radiologists*

The results of the comparison between the deep learning system and radiologists are also shown in [Table 1](#). The radiologists' performance demonstrated an accuracy of 81.2%, sensitivity of 80.2%, specificity of 82.0%, a positive predictive value of 78.7%, and a negative predictive value of 83.4%. The deep learning system showed slightly higher performance values than the radiologists, with significant differences in specificity (Mann-Whitney U test; AlexNet *vs* radiologists,  $p = 0.0445$ ; GoogleNet *vs* radiologists,  $p = 0.0424$ ).

The results of the ROC analyses are shown in [Figure 4](#). The AUCs of the deep learning systems using AlexNet and GoogleNet were 0.87 and 0.85 respectively, while that of the radiologists was 0.74. There was a statistically significant difference between the AUC values of the deep learning systems and the radiologists ( $\chi^2$  test; AlexNet *vs* radiologists,  $p < 0.0001$ ; GoogleNet *vs* radiologists,  $p = 0.0003$ ).

## Discussion

Recently, with the development of deep learning systems, artificial intelligence has been applied to a number of medical fields.<sup>11–16</sup> Among the architectures

used for deep learning models, convolutional neural networks with multiple layers are especially suitable for imaging diagnosis, because they are able to take advantage of local connections, shared weights, pooling and preferred analysis.<sup>15,18</sup> When image data are input into the top layer, learning of the correct classification occurs through the transmission of information through the layers, with the model performing output of the proposed classification in the final layer.<sup>13,16</sup> The system is able to learn adaptive image features and perform image classification simultaneously, without requiring input of predefined imaging features for a specific recognition task.<sup>14,15</sup> Although deep learning systems have been applied to various medical fields, they have not yet been widely applied to dental fields. Therefore, as a trial application in the endodontic field, we examined the performance of a deep learning system for evaluating the number of distal roots of mandibular first molars on panoramic radiographs.

Knowledge of the variations in root canal morphology is a clinically important factor for proper endodontic treatment.<sup>7</sup> Additional disto-lingual roots are thought to be a major anatomical variant in the mandibular first molars.<sup>2,7</sup> The differences in occurrence of the root variations might be attributable to racial and ethnic differences.<sup>2,3,7</sup> For example, European populations show a less than 5% occurrence rate for disto-lingual roots,<sup>3,5,9</sup> and other studies have reported 5.7% in an Indian subpopulation,<sup>4</sup> 3.1% in an Iranian population,<sup>7</sup> and less than 5% in the Brazilian population.<sup>5</sup> However, occurrence rates of 23.6% for a Japanese population<sup>6</sup> and 22.1% for a Chinese population.<sup>2</sup> These occurrence rates are higher than those reported from other populations.<sup>3–5,7,9</sup> The present study showed an occurrence rate of 21.4%, which is consistent with other reports on East-Asian subjects.<sup>2,6</sup>

Vertucci observed specimen teeth using a dissecting microscope and created a classification system according to the root canal configuration.<sup>19</sup> Vertucci found that the most common configurations of the root canals in the mesial and distal roots were types IV and I respectively.<sup>19</sup> Many studies on the three-dimensional classification of root canal configurations on CBCT have been performed, and they have reported similar trends in frequency.<sup>1–5,7,8</sup> The application of deep learning system to evaluation of this root canal morphology should be conducted in future research.

Some methods were adopted on practice of the deep learning system. The diagnostic performance of the deep learning system depends on the quality and bias of the input image data. Imbalances in the sample should be avoided during the training process,<sup>20</sup> and multifold cross-validation was therefore used to eliminate any bias in the training and testing datasets.<sup>20</sup> A very substantial quantity of training data is required to create a learning model, because the performance of a deep learning system depends on both the quality and quantity of the training dataset.<sup>12</sup> When the data quantity available for

training is insufficient, a data augmentation strategy may be applied.<sup>13,20</sup> The strategy of using multiple image patches from the same patient allowed us to generate a large number of imaging tensors upon which the algorithm could be trained.<sup>21</sup> Although we prepared more than 11,000 image patches for each group after data augmentation, the total quantity of training dataset available for each cross-validation may still be considered small. In particular, a larger quantity of data will be needed if a study is to focus on the dental characteristics of a specific population.<sup>12,21</sup>

The deep learning system was shown to have high performance in determining the number of distal roots. The accuracy, sensitivity, and specificity of the deep learning system using AlexNet were 87.4, 77.3, and 97.1% respectively, while with GoogleNet they were 85.3, 74.2, and 95.9% respectively. In this study, we compared the performance of AlexNet and GoogleNet in the classification task. AlexNet consists of five convolution layers and three fully-connected layers, whereas GoogleNet has 22 layers.<sup>17,22,23</sup> GoogleNet takes longer to train, but its diagnostic performance is considered to be high.<sup>22,23</sup> Sugimori showed that the performance of both CNNs fluctuated according to the size of the training datasets.<sup>22</sup> This may explain why there was no significant difference in the diagnostic performance of these two CNNs in this study. The two CNNs were able to achieve similar or superior diagnostic performance to radiologists with more than 20 years of experience.

The deep learning system may have value in diagnostic practice.<sup>12</sup> Image classification by a deep learning system could assist inexperienced doctors in the interpretation of images. However, the clinical use of this system still presents some challenges.<sup>15</sup> In this study, the image patches were created by manual segmentation, and this procedure required substantial time. Once the image patches were created, it took only a short time for the system to learn the categorization. In this study, the learning procedure took 51 min with 200 epochs, and the testing procedure took 9 sec using AlexNet. Therefore, the clinical application of deep learning systems is still subject to many challenges, with the development of automatic segmentation techniques being a priority.<sup>24</sup>

Another point worthy of consideration is the optimal size of the image patches. The patch size should be chosen so that it focuses on a small region without including too much of the surroundings; this will help ensure that the system generalizes the texture patterns of the specific tissues of interest.<sup>21</sup> Patches that are too small may not provide enough anatomical information, while patches that are too large may result in high training errors because of misleading information from the surroundings.<sup>21</sup> In this study, the image patches were fixed at a size sufficient to contain the tooth roots while not being too large.

This study did not examine age-related morphological variations. Gani *et al* investigated the age-related morphological changes in the mesial root canals of the mandibular first molars.<sup>25</sup> However age-related fluctuation in the number of distal roots has not been reported. Most of our subjects were young adults, and further surveys in children and older adults are required.

The distal root canal may present with curvature,<sup>8</sup> and the disto-lingual root canal shows various degree of curvature.<sup>2</sup> The complex morphology of the canals may make cleaning and shaping procedures more difficult, but awareness of the morphology may prevent perforation or stripping.<sup>8</sup> Further studies on root canal curvature will therefore also be necessary.

In this study, we used CBCT findings as the gold standard for the classification. As the root canal morphology of vital teeth cannot be evaluated microscopically, it is most likely to be determined on the basis of CBCT, and this can be done with high accuracy.<sup>5,7,8</sup> However, it is not possible to perform CBCT on all patients undergoing root canal treatment. If root canal morphology could be predicted on panoramic and periapical radiographs before treatment, it would be possible to identify those patients who require CBCT. In addition, this study verified that the deep learning system was equivalent or even slightly better than the trained radiologists in respect to identifying the presence of an extra root or not in the distal root of mandibular first molars.

The deep learning was performed with panoramic radiographs that are easy to obtain from healthy patients. This study is one of a series of studies aimed at using deep learning artificial intelligence to automate diagnoses on panoramic radiography. In the future, the deep learning system should be applied to periapical radiography, which is considered indispensable for endodontics treatment.<sup>8</sup> If this was to be undertaken, it is expected that the classification of root canal morphology would be improved.

## Conclusion

In conclusion, the number of distal roots in mandibular first molars was evaluated using CBCT. Learning models were created by extracting image patches from panoramic radiographs and inputting them into deep learning systems. The deep learning systems showed high levels of performance in differentiating whether the distal root was single or with an extra root.

## Acknowledgment

We thank Karl Embleton, from Edanz Group ([www.edanzediting.com/ac](http://www.edanzediting.com/ac)) for editing a draft of this manuscript.

## References

1. Madani ZS, Mehraban N, Moudi E, Bijani A. Root and canal morphology of mandibular molars in a selected iranian population using cone-beam computed tomography. *Iran Endod J* 2017; **12**: 143–8. doi: <https://doi.org/10.22037/iej.2017.29>
2. Zhang X, Xiong S, Ma Y, Han T, Chen X, Wan F, et al. A Cone-beam computed tomographic study on mandibular first molars in a chinese subpopulation. *PLoS One* 2015; **10**: e0134919. doi: <https://doi.org/10.1371/journal.pone.0134919>
3. Celikten B, Tufenkci P, Aksoy U, Kalender A, Kermeoglu F, Dabaj P, et al. Cone beam CT evaluation of mandibular molar root canal morphology in a turkish cypriot population. *Clin Oral Investig* 2016; **20**: 2221–6. doi: <https://doi.org/10.1007/s00784-016-1742-2>
4. Felsypremila G, Vinothkumar TS, Kandaswamy D. Anatomic symmetry of root and root canal morphology of posterior teeth in Indian subpopulation using cone beam computed tomography: A retrospective study. *Eur J Dent* 2015; **9**: 500–7. doi: <https://doi.org/10.4103/1305-7456.172623>
5. Caputo BV, Noro Filho GA, de Andrade Salgado DM, Moura-Netto C, Giovani EM, Costa C. Evaluation of the root canal morphology of molars by using cone-beam computed tomography in a brazilian population: part I. *J Endod* 2016; **42**: 1604–7. doi: <https://doi.org/10.1016/j.joen.2016.07.026>
6. Ogawa A, Seki S. Evaluation of root anatomy and root canal configurations of mandibular first molars using dental cone-beam computed tomography. *JJE* 2017; **38**: 93–8.
7. Rahimi S, Mokhtari H, Ranjkesh B, Johari M, Frough Reyhani M, Shahi S, et al. Prevalence of extra roots in permanent mandibular first molars in iranian population: A CBCT analysis. *Iran Endod J* 2017; **12**: 70–3. doi: <https://doi.org/10.22037/iej.2017.14>
8. Torres A, Jacobs R, Lambrechts P, Brizuela C, Cabrera C, Concha G, et al. Characterization of mandibular molar root and canal morphology using cone beam computed tomography and its variability in Belgian and Chilean population samples. *Imaging Sci Dent* 2015; **45**: 95–101. doi: <https://doi.org/10.5624/isd.2015.45.2.95>
9. Ceperuelo D, Lozano M, Duran-Sindreu F, Mercadé M. Root canal morphology of chalcolithic and early bronze age human populations of El mirador cave (Sierra de Atapuerca, Spain). *Anat Rec* 2014; **297**: 2342–8. doi: <https://doi.org/10.1002/ar.22958>
10. Wrzesień M, Olszewski J. Absorbed doses for patients undergoing panoramic radiography, cephalometric radiography and CBCT. *Int J Occup Med Environ Health* 2017; **30**: 705–13. doi: <https://doi.org/10.13075/ijom.1896.00960>
11. Song Q, Zhao L, Luo X, Dou X. Using deep learning for classification of lung nodules on computed tomography images. *J Healthc Eng* 2017; **2017**: 1–7. doi: <https://doi.org/10.1155/2017/8314740>
12. Xue Y, Zhang R, Deng Y, Chen K, Jiang T. A preliminary examination of the diagnostic value of deep learning in hip osteoarthritis. *PLoS One* 2017; **12**: e0178992. doi: <https://doi.org/10.1371/journal.pone.0178992>
13. Wang H, Zhou Z, Li Y, Chen Z, Lu P, Wang W, et al. Comparison of machine learning methods for classifying mediastinal lymph node metastasis of non-small cell lung cancer from <sup>18</sup>F-FDG PET/CT images. *EJNMMI Res* 2017; **7**: 11. doi: <https://doi.org/10.1186/s13550-017-0260-9>
14. Byrne MF, Chapados N, Soudan F, Oertel C, Linares Pérez M, Kelly R, et al. Real-time differentiation of adenomatous and hyperplastic diminutive colorectal polyps during analysis of unaltered videos of standard colonoscopy using a deep learning model. *Gut* 2017; 2017:314547. doi: <https://doi.org/10.1136/gutjnl-2017-314547>
15. Wang X, Yang W, Weinreb J, Han J, Li Q, Kong X, et al. Searching for prostate cancer by fully automated magnetic resonance imaging classification: deep learning versus non-deep learning. *Sci Rep* 2017; **7**: 15415. doi: <https://doi.org/10.1038/s41598-017-15720-y>
16. Lee H, Tajmir S, Lee J, Zissen M, Yeshiwas BA, Alkasab TK, et al. Fully automated deep learning system for bone age assessment. *J Digit Imaging* 2017; **30**: 427–41. doi: <https://doi.org/10.1007/s10278-017-9955-8>
17. Krizhevsky A, Sutskever I, Hinton GE. Imagenet classification with deep convolutional neural networks. *Adv Neural Inf Process Syst* 2012; **25**: 1–9.
18. Gao XW, Hui R, Tian Z. Classification of CT brain images based on deep learning networks. *Comput Methods Programs Biomed* 2017; **138**: 49–56. doi: <https://doi.org/10.1016/j.cmpb.2016.10.007>
19. Vertucci FJ. Root canal anatomy of the human permanent teeth. *Oral Surg Oral Med Oral Pathol* 1984; **58**: 589–99. doi: [https://doi.org/10.1016/0030-4220\(84\)90085-9](https://doi.org/10.1016/0030-4220(84)90085-9)
20. Xue Y, Chen S, Qin J, Liu Y, Huang B, Chen H. Application of deep learning in automated analysis of molecular images in cancer: A survey. *Contrast Media Mol Imaging* 2017; **2017**: 1–10. doi: <https://doi.org/10.1155/2017/9512370>
21. Trebeschi S, van Griethuysen JJM, Lambregts DMJ, Lahaye MJ, Parmar C, Bakers FCH, et al. Deep learning for fully-automated localization and segmentation of rectal cancer on multiparametric MR. *Sci Rep* 2017; **7**: 5301. doi: <https://doi.org/10.1038/s41598-017-05728-9>
22. Sugimori H. Classification of computed tomography images in different slice positions using deep learning. *J Healthc Eng* 2018; **2018**: 1753480–. doi: <https://doi.org/10.1155/2018/1753480>
23. Lam C, Yi D, Guo M, Lindsey T. Automated detection of diabetic retinopathy using deep learning. *AMIA Jt Summits Transl Sci Proc* 2017; **2018**: 147–55.
24. Zhao X, Wu Y, Song G, Li Z, Zhang Y, Fan Y. A deep learning model integrating FCNNs and CRFs for brain tumor segmentation. *Med Image Anal* 2018; **43**: 98–111. doi: <https://doi.org/10.1016/j.media.2017.10.002>
25. Gani OA, Boiero CF, Correa C, Masin I, Machado R, Silva EJ, et al. Morphological changes related to age in mesial root canals of permanent mandibular first molars. *Acta Odontol Latinoam* 2014; **27**: 105–9. doi: <https://doi.org/10.1590/S1852-48342014000300001>